Modeling and Nonlinear Control of Two-Wheeled Self-Balancing Human Transporter

Article *in* Journal of Applied Nonlinear Dynamics · June 2020

DOI: 10.5890/JAND.2021.03.002

4 authors:

Mohit Makkar
The LNM Institute of Information Technology
12 PUBLICATIONS **11** CITATIONS
SEE PROFILE

Saransh Jain
The LNM Institute of Information Technology
5 PUBLICATIONS **15** CITATIONS
SEE PROFILE

Sarthak Jain
The LNM Institute of Information Technology
3 PUBLICATIONS **0** CITATIONS
SEE PROFILE

Deepak Rajendra Unune
The LNM Institute of Information Technology
77 PUBLICATIONS **808** CITATIONS
SEE PROFILE

Journal of Applied Nonlinear Dynamics

Modeling and Nonlinear Control of Two-Wheeled Self-Balancing Human Transporter

--Manuscript Draft--

Manuscript Number:	JAND-D-19-00051R3
Article Type:	Regular Research Paper
Full Title:	Modeling and Nonlinear Control of Two-Wheeled Self-Balancing Human Transporter
Abstract:	The two-wheeled self-balancing human transporters (TW-SBHT) are being widely used in transportation. Being a complex and nonlinear system, the control problem of TW-SBHT is a challenging task and needs to be tackled to achieve the control objectives of maintaining uniform speed and dynamic stability. In this work, a non-linear control i.e. State-Dependent Riccati Equation (SDRE) has been implemented for effective control of TW-SBHT and its performance is compared with the linear controls including Proportional-Integral-Derivative (PID) and Linear-Quadratic Regulator (LQR) techniques. The application of SDRE for control of TW-SBHT has been presented and its performance is compared with linear control strategies.
Corresponding Author:	Mohit Makkar, Ph.D The LNMIIT INDIA
Other Authors:	Saransh Jain, B.Tech
	Sarthak Jain, B.Tech
	Deepak Rajendra Unune
Keywords:	self-balancing human transporters; modeling; control; SDRE

Journal of Applied Nonlinear Dynamics 1(1) (2012) 1-6

Journal of Applied Nonlinear Dynamics

https://lhscientificpublishing.com/Journals/JAND-Default.aspx

Modeling and Nonlinear Control of a Two-Wheeled Self Balancing Human Transporter

Saransh Jain [a], Mohit Makkar [a] †, Sarthak Jain[a], Deepak Unune [b].

[a]Department of Mechanical-Mechatronics Engineering, The LNM Institute of Information Technology Jaipur, 302031, India

[b]Department of Materials Science and Engineering, University of Sheffield, INSIGNEO Institute for in silico Medicine, The Pam Liversidge Building, Sheffield, S1 3JD, United Kingdom.

Submission Info

Communicated by Referees
Received DAY MON YEAR
Accepted DAY MON YEAR
Available online DAY MON YEAR

Keywords

self-balancing human transporters
modeling
control
SDRE

Abstract

The two-wheeled self-balancing human transporters (TW-SBHT) are being widely used in transportation nowadays owing to their advantages such as energy saving, environmental protection, simple structure, and flexible operation. The modelling and control of TW-SBHT have emerged as one of the trending research areas in the field of control system design of mobile robots. Being a complex and nonlinear system, the control problem of TW-SBHT is a challenging task and needs to be effectively tackled to achieve the control objectives of maintaining uniform speed and dynamic stability. Though linear control strategies for TW-SBHT have been already proposed in the literature, they cannot offer an effective control for large external disturbances. Therefore, in this work, a non-linear control i.e. State-Dependent Riccati Equation (SDRE) has been implemented for effective control of TW-SBHT and its performance is compared with the linear controls including Proportional-Integral-Derivative (PID) and Linear-Quadratic Regulator (LQR) techniques. Initially, the more accurate model of TW-SBHT has been derived by applying the suitable modifications in existing models. Then, the application of SDRE for control of TW-SBHT has been presented and its performance is compared with linear control strategies.

1 Introduction

Over the past few years, the studies on mobile wheeled inverted pendulum models have attracted the curiosity of researchers across the world because of their high navigation capabilities. The two-wheeled self-balancing human transporter (TW-SBHT), like Segway, is a mobile robot with a highly unstable system. Its platform is required to be controlled to maintain the appropriate balance of the vehicle

†Corresponding author
Email address: saransh.j1997@gmail.com, mohit.makkar@lnmiit.ac.in, sarthakjain098@gmail.com and deepunune@gmail.com

ISSN 2164-6457, eISSN 2164-6473/$-see front materials

and the driver. TW-SBHT contains a driving lever, one horizontal platform, and wheels which are driven by electric motors. The driver stands on the horizontal platform. TW-SBHT can move forward, backward and turn in either left or right direction. Unlike the scooter, whose wheels are connected in series and are interdependent, the TW-SBHT has wheels in a parallel configuration. The lever gives support to the driver and helps in steering the vehicle. TW-SBHT is controlled by the driver$'s$ motion. When the driver leans his/her body in the forward direction, it moves forward. Similarly, when the driver leans in the backward direction, it moves backward. If the lever is kept standstill, then the vehicle comes to rest, i.e. it works as a braking system. The lever of the TW-SBHT is also working as the speed controller where a greater the deflection in the lever angle yields a greater velocity. Any deflection in the lever angle is nullified by the motion of the TW-SBHT in the corresponding direction of the deflection, using driving motors.

TW-SBHT is based on the dynamics of the inverted pendulum. The inverted pendulum is generally considered as an unstable and highly non-linear system. The dynamics of the TW-SBHT is complex and nonlinear as compared to the system dynamics of an inverted pendulum. It is also very difficult to control the system with uncertain parameters and states. Over the years, the control labs across the world have been inventing new and innovative control algorithms and implemented them on TW-SBHT. Shimizu et al. [1] implemented the PID based tilt control movement control for the two-wheeled inverted pendulum. Lin et al. [2] implemented the teaching of feedback control concepts for self-balancing human transportation vehicle to maintain the vehicle without falling and to achieve the desired yaw rate tracking. Lupian et al. [3] designed the Linear Quadratic Gaussian (LQG) controller with a Kalman-Bucy estimator for better stabilization of TW-SBHT. Huang et al. [4] applied the two Sliding Mode Control on the inverted pendulum system for velocity control problem. Irfan et al. [5] implemented the advanced sliding mode control (ASMC) technique and compared the performance of ASMC with the LQR and sliding mode control (SMC) on the various test signals. They performed the analysis on the basic of chattering, less settling time and small steady state error. Lin et al. [6] implemented the adaptive robust controller on the TW-SBHT. However, all the control scheme mentioned above are the linear controllers. Such controllers offer a significant performance only when the parameters of the systems are constant, and the system dynamics are linear for approximately a small deflection angle around the equilibrium point. Typically, for large pitch angle deflection which is due to intentional maneuvers or external disturbances, the TW-SBHT behaviour is in the nonlinear region, and for such instances, the linear controller$'s$ results are not promising [7]. Application of nonlinear controllers can overcome such problems and improve the driving performance. Xu et al. [8] implemented the integral sliding mode controller on the two-wheeled mobile robots. Li et al. [9] proposed the nonlinear control design for TW-SBHT. They developed an output feedback adaptive neural network controller. Huang. et al. [10] presented the fuzzy control scheme on the two-wheeled inverted pendulum.

To overcome the limitation of linear controls and completely realize the agile movements of the TW-SBHT, it is essential to employ the dynamic characteristics into the model-based control design. To address this issue, in this work, the State-Dependent Riccati Equation (SDRE) has been employed to the TW-SBHT control problem. The SDRE control has the benefit of utilizing the non-linear system dynamics directly in the LQR like optimal control design. In this control design, the system dynamics is represented as the state dependent coefficient (SDC) matrices which are nothing but a linear looking form of the non-linear system. The SDC formation is also known as extended linearization or pseudo linearization. The formation of the SDC matrix is the most critical issue in the SDRE controller. However, the SDC provides flexibility in the control design fetching the optimal gains. In SDRE, the cost function is used to handle the optimal tracking problem for the desired trajectories. Then, the SDRE method is used to find the sub-optimal solution of the optimal tracking problem. It provides the approximate solution of the optimal tracking problem which avoids the arising of the Hamilton-Jacobi-Bellman (HJB) which is highly complex and almost impossible to solve. [11]. SDRE control

technique offers ease of computing as compared to other nonlinear controllers. More importantly, it retains the nonlinearities of the system. The SDRE, being a classical nonlinear control approach, has been already successfully applied in the automobile and aviation industries [12]. . Therefore, in this work, the implementation of SDRE to control the TW-SBHT has been proposed.

In this work, initially, a better dynamic model for TW-SBHT is proposed and then, the SDRE has been implemented to control it.. The first objective of the control design was to maintain the lever or pitch angle (ψ) at a specific angle so that TW-SBHT can move with constant velocity, which is generally required while traveling. The second objective is to stabilize the lever at an upright position at zero degrees. To overcome the performance limit of linear control in the large external disturbances.The performance of the nonlinear controller is compared with the linear controller by given a step input of (12.8) degree as an external disturbance. The system has inherent uncertainties like driver$'s$ mass and inertia is not investigated here.

2 Mathematical Modeling

Table 1 Parameters of the system

Parameters	Symbol	Units
Gravitational constant	g = 9.81	m/s^2
Wheel weight	m = 4.6	Kg
Radius of wheel	$R_w = 0.24$	meter
Wheel inertia	$J_w = mR_w^2$	Kgm^2
Transporter body weight	$M_v = 30.05$	Kg
Mass of Driver	$M_r = 80$	Kg
Total Mass	M=$M_r + M_v$	Kg
Body height	H=-0.03	metre
Length of Driver	$L_r = 1.8$	metre
Distance between the centre of mass and wheel axle	L=0.7155	metre
Inertia of Driver	$J_r = M_r L^2/3$	Kgm^2
Body pitch Inertia	$J_b = 87.89$	Kgm^2
Inertia of DC motor	$J_m = 0.0075$	Kgm^2
Resistance of motor	$R_m = 14$	Ω
Back EMF constant of DC motor	$K_b = 0.72$	Vs/rad
Torque constant of DC motor	$K_t = 0.833$	Nm/A
Gear Ratio of DC motor	n= 14	-
Friction coefficient between axle and bearings	F_m=0.3	-
Friction between Tyres and ground	f_w=0.5	-
Input voltage	V=24	Volt

In this section, the mathematical modelling of the TW-SBHT is presented. The model is not derived from scratch but rather selected after analysing the various existing models. Then the suitable modification is applied in these previous models. The Yamamoto et al [13]derived the model using the Lagrangian mechanics and considered the yaw angle. However, the model presented in this work neglects the yaw angle. The equation of motion derived by Arvidsson et al [14].14 is very close to the real system but they neglected the rolling friction between the tires and ground. The dynamics

of the TW-SBHT derived by Lin et al. [6] considered the rolling friction and the viscous friction. However, they neglected the inertia of motor which is a crucial parameter. The viscous friction and rolling friction have been incorporated while deriving the dynamics of TW-SBHT in this work. The rolling friction is friction between the tires and ground (cemented road). Here, the rolling friction coefficient is assumed as the constant with the time. It was also assumed that the wheels are always with the floor and no slipping is occur between the wheels and the floor i.e. pure rolling is occuring. The steering of the TW-SBHT i.e. the yaw angle, is neglected while deriving the equation of motion. Nevertheless, all other crucial parameters like the inertia of motor are considered by due analysis. The considered system is two degree of freedom system. The TW-SBHT is an underactuated system because TW-SBHT has two degree of freedom i.e. pitch angle (ψ) of the driving lever and average angle (θ) of the corresponding wheel but only one is actuated i.e. angular displacement of wheel (θ). The TW-SBHT model parameters adapted from [14] and coordinates are presented in Table (2) and Table (2), respectively. The kinematic constraints of the system were derived while assuming the no vertical motion in Z direction as shown in Fig.1.

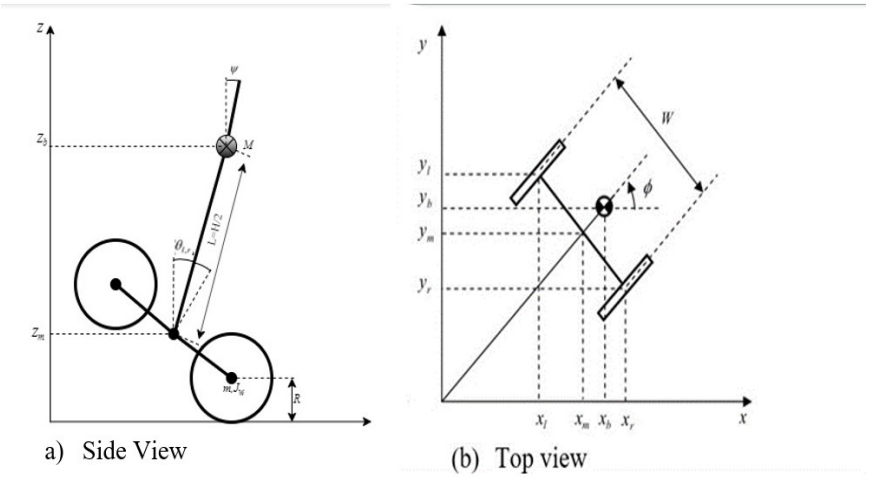

Fig. 1 Coordinate system of TW-SBHT (a) Side View and (b) Top View

Table 2 Coordinates of the system

Symbols	Units
x_l, y_l, z_l	Position coordinates of left wheel
x_r, y_r, z_r	Position coordinates of right wheel
x_b, y_b, z_b	Position coordinates of centre of mass
θ_l, θ_r	Angular displacement of left and right wheel respectively
θ_{lm}, θ_{rm}	Angular displacement of left and right wheel respectively

The kinematic constraints equations are:

$$\ddot{x}cos(\psi) + \ddot{(}y)sin(\psi) = R\ddot{\theta}_l + w\ddot{\psi} \tag{1}$$

$$\ddot{x}cos(\psi) + \ddot{(}y)sin(\psi) = R\ddot{\theta}_r + w\ddot{\psi} \tag{2}$$

$$\dot{y}cos(\psi) - \dot{(}x)sin(\psi) = 0 \tag{3}$$

Where $\dot{\theta}$ and $\dot{\psi}$ are the linear velocities along the x and y direction respectively.$\ddot{\theta}_l$ is the angular acceleration of the left wheel and $\ddot{\theta}_r$ is the angular acceleration of the right wheel.

The expression of the total energy is derived based on the Lagrangian function. The total energy can be written as the sum of Translation kinetic energy (T1), rotational kinetic energy (T2) and potential energy (U):

$$T_1 = \frac{1}{2}m(\dot{x}_l^2 + \dot{y}_l^2 + \dot{z}_l^2) + \frac{1}{2}m(\dot{x}_r^2 + \dot{y}_r^2 + \dot{z}_r^2) + \frac{1}{2}M(\dot{x}_b^2 + \dot{y}_b^2 + \dot{z}_b^2) \tag{4}$$

$$T_2 = \frac{1}{2}J_W\dot{\theta}_l^2 + \frac{1}{2}J_W\dot{\theta}_r^2 + \frac{1}{2}J_W\dot{\psi}^2 + \frac{1}{2}nJ_m(\dot{\theta}_l - \dot{\psi})^2 + \frac{1}{2}n^2J_m(\dot{\theta}_r - \dot{\psi})^2 \tag{5}$$

$$U = mgz_l + mgz_r + Mgz_b \tag{6}$$

Coordinates can be expressed as:

$$(x_m, y_m, z_m) = (\int R_w\dot{\theta}dt, 0, R_w) \tag{7}$$

$$(x_l, y_l, z_l) = (x_m, \frac{W}{2}, z_m) \tag{8}$$

$$(x_r, y_r, z_r) = (x_m, -\frac{W}{2}, z_m) \tag{9}$$

$$(x_b, y_b, z_b) = (x_m + Lsin(\psi), y_m, z_m + Lcos(\psi) \tag{10}$$

By putting the Lagrangian L in the Lagrangian function Eq. (11) and Eq. (12):

$$\frac{d}{dt}(\frac{\partial L}{\partial \dot{\theta}}) - (\frac{\partial L}{\partial \theta}) = F_\theta \tag{11}$$

$$\frac{d}{dt}(\frac{\partial L}{\partial \dot{\psi}}) - (\frac{\partial L}{\partial \psi}) = F_\psi \tag{12}$$

By solving Eq. (11) and Eq. (12) the two equations of motion which governs the TW-SBHT, can be written as Eq. (13) and Eq. (14):

$$((2m+M)R_w^2 + 2J_w + 2n^2J_m)\ddot{\theta} + (MLR_wcos(\psi) - 2n^2J_m)\ddot{\psi} - MLR_w\dot{\psi}^2sin(\psi) = F_\theta \tag{13}$$

$$(MLR_wcos(\psi) - 2n^2J_m)\ddot{\theta} + (ML^2 + J_b + 2n^2J_m)\ddot{\psi} - MgLsin(\psi) = F_\psi \tag{14}$$

2.1 Actuator model

The DC motor is used in the TW-SBHT due to its simplicity and the capability. The two parallel wheels are operated with the two BLDC motor.

The generalized forces F_θ and F_ψ are calculated by considering the DC motor torque, viscous friction between the body and motor axle, and the friction between the wheels and ground. The inductance of the motor is neglected because the electric time constant which is much smaller than the mechanical time constant [13]. By applying Kirchhoff$'s$ Law on the DC motor, the final equations of F_θ and F_ψ were obtained:

$$F_\theta = a(V) - 2(b + F_w)\dot{\theta} + 2b\dot{\psi} \tag{15}$$

$$F_\psi = -a(V) + 2b\dot{\theta} - 2b\dot{\psi} \tag{16}$$

$$a = \frac{nK_t}{R_m} \tag{17}$$

$$b = \frac{nK_tK_b}{R_m} + F_m \tag{18}$$

Now, substituting Eq. (15) and Eq. (16) into Eq. (13) and Eq. (14).Then the equations are solved for the angular acceleration of wheel $\ddot{\theta}$ and the angular acceleration of the driving lever $\ddot{\psi}$,comes out to be:

$$\begin{aligned}\ddot{\theta} = (&J_bVa + 2J_bb\dot{\psi} - 2J_bb\dot{\theta} - 2J_bF_w\dot{\theta} + L^2MVa + 2L^2Mb\dot{\psi} - 2L^2Mb\dot{\theta} - 2L^2MF_w\dot{\theta} - 4J_mF_wn^2\dot{\theta} \\ &+L^3M^2R_w\dot{\psi}^2sin(\psi) - L^2M^2R_wgcos(\psi)sin(\psi) + J_bLMR_w\dot{\psi}^2sin(\psi) + 2J_mLMgn^2sin(\psi) + LMR_wVacos(\psi) \\ &+2LMR_wb\dot{\psi}cos(\psi) - 2LMR_wb\dot{\theta}cos(\psi) + 2J_mLMR_wn^2\dot{\psi}^2sin(\psi))/(2J_bJ_w + L^2M^2R_w^2 + 2J_wL^2M + J_bMR_w^2 \\ &+2J_bJ_mn^2 + 4J_mJ_wn^2 + 2J_bR_w^2m + 2J_mL^2Mn^2 + 2J_mMR_w^2n^2 + 2L^2MR_w^2m + 4J_mR_w^2mn^2 - L^2M^2R_w^2cos(\psi)^2 \\ &+4J_mLMR_wn^2cos(\psi))\end{aligned}$$

$$\begin{aligned}\ddot{\psi} = -(&2J_wVa + 4J_wb\dot{\psi} - 4J_wb\dot{\theta} + MR_w^2Va + 2MR_w^2b\dot{\psi} - 2MR_w^2b\dot{\theta} + 2R_w^2Vam + 4R_w^2bm\dot{\psi} + 4J_mf_wn^2\dot{\theta} \\ &-4R_w^2bm\dot{\theta} - LM^2R_w^2gsin(\psi) - 2J_wLMgsin(\psi) - 2J_mLMgn^2sin(\psi) - 2LMR_w^2gmsin(\psi) + LMR_wVacos(\psi) \\ &+L^2M^2R_w^2\dot{\psi}^2cos(\psi)sin(\psi) + 2LMR_wb\dot{\psi}cos(\psi) - 2LMR_wb\dot{\theta}cos(\psi) - 2LMR_wf_w\dot{\theta}cos(\psi) \\ &-2J_mLMR_wn^2\dot{\psi}^2sin(\psi))/(2J_bJ_w + L^2M^2R_w^2 + 2J_wL^2M + J_bMR_w^2 + 2J_bJ_mn^2 + 4J_mJ_wn^2 + 2J_bR_w^2m + 2J_mL^2Mn^2 + \\ &2J_mMR_w^2n^2 + 2L^2MR_w^2m + 4J_mR_w^2mn^2 - L^2M^2R_w^2cos(\psi)^2 + 4J_mLMR_wn^2cos(\psi)).\end{aligned}$$

3 Controller Design

The TW-SBHT is designed to use the closed loop controller for the speed control and the balancing of the lever. The motive of the control design was to stabilize the lever so that the rider does not fall off from the vehicle and to control the speed of TW-SBHT. Here, the objective is to bring the TW-SBHT to a constant speed by maintaining the constant deflection in the lever after the initial deflection.

3.1 PID-PID Controller

The PID-PID controller is applied to the state which plays an important role in stabilizing the system and works according to the control design. The purpose of the first PID was to control the pitch angle of the lever while the second was to control the wheels speed. The PID-PID control is applied to the full non-linear system, and a Simulink model is designed for this purpose. In this control design, the external disturbance is not included. The states used during the control design are:

1. The initial pitch angle of the lever is taken to be as 18° which finally becomes 6°.
2. The initial wheel velocity is set to be 0 rad/sec and the final values are set to be 0.28 rad/sec. When the pitch angle achieves the desired value i.e. 6 °, at the same time the value of wheel velocity becomes constant that is 0.28 rad/sec.

The simulation was performed in MATLAB, and the results are plotted for four states of the system.(θ $\dot{\theta}$ ψ and $\dot{\psi}$) all the inferences from the simulation are presented in Fig. 2, Fig. 3, Fig. 4 and Fig. 5. The initial deflection in pitch angle (ψ) of 18° in the forward direction, demands the sudden

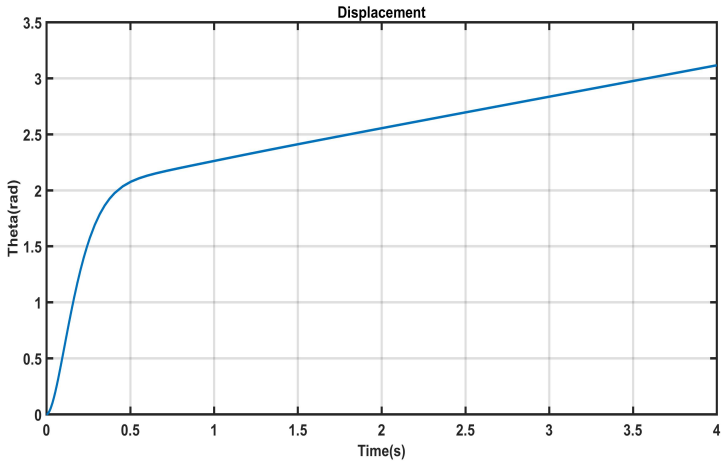

Fig. 2 PID-PID: Displacement

change in the velocity in a forward direction. This generates the huge notch in the graph of velocity as shown in Fig. 3. In order to achieve the final value of the pitch angle of 6°, the TW-SBHT moves in a forward direction to minimize the error in the angle between the desired and the actual values of the deflections. As soon as the pitch angle (ψ) converges to the desired angle. Correspondingly, the velocity of TW-SBHT attains the constant speed of 0.28 rad/s. With the above simulation results, it can be claim that PID-PID control technique works effectively. The PID-PID controller works according to the control design strategy and fulfills all the control design goals.

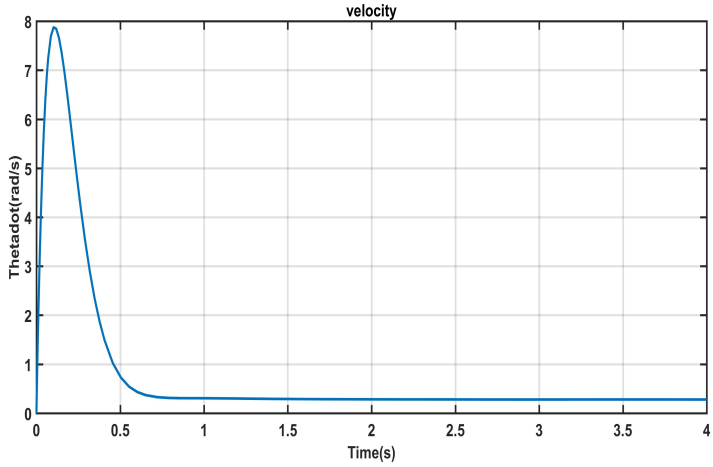

Fig. 3 PID-PID: Velocity

4 LQR controller

Generally, the LQR control is used to provide the optimal solution for a given constraint. The LQR generates a control action which made the process (plant) stable. At the same time LQR also cancels out the effect of external disturbances. The optimum performance of LQR is determined by minimizing the cost function. The problem statement is to locate and optimize the given system at a value or to

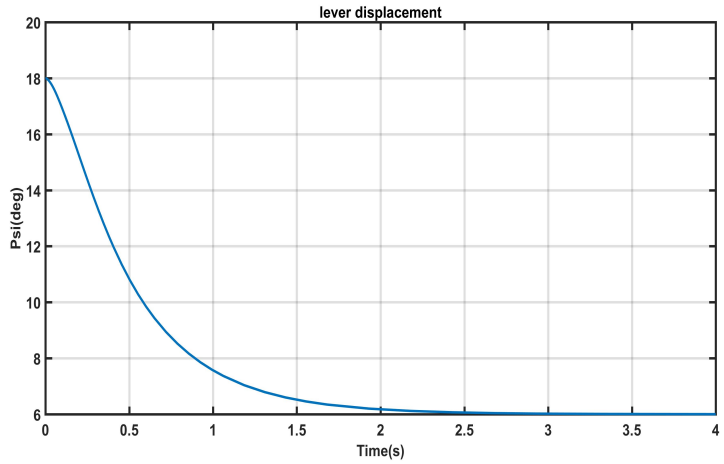

Fig. 4 PID-PID: Lever Displacement

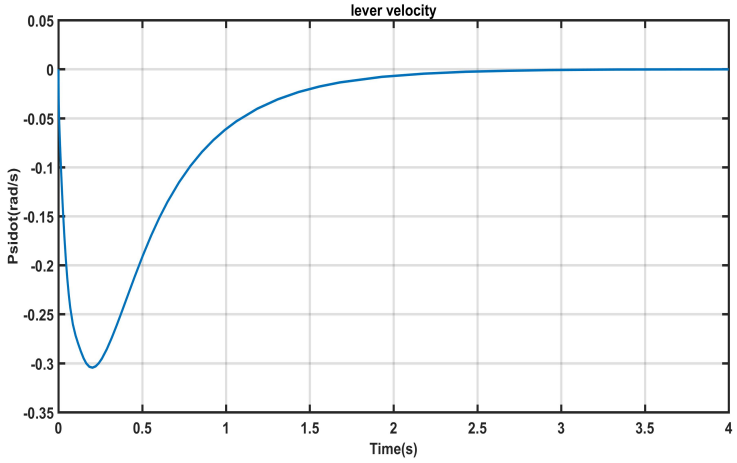

Fig. 5 PID-PID: Lever Velocity

follow some state variable and simultaneously get the maximum value of (PI) by various tests [15].

The LQR controller is the optimal version of the pole placement method. The LQR controller provides the best control law which moves the system to the desired eigenvalue [16]. In order to get the system matrices A and B, linearization is applied on the full nonlinear system at the operating point $x = [0,0,0,0]$. The initial values of all the four states (θ $\dot{\theta}$ ψ and $\dot{\psi}$) are taken as $x_0 = [0,0,\pi/10,0]^T$. The rank of the controllability matrix (A, B) 4 which shows that the system is controllable. The linear state space is obtained as:

$$\dot{x} = Ax - Bu \tag{19}$$

where

$$x = [\theta, \dot{\theta}, \psi, \dot{\psi}]^T. \tag{20}$$

The full state feedback controller,$U = -Kx$ where K is the gain matrix. K is computed by minimizing the cost function. The cost function indicates how bad the system is if states are not at the reference state.

$$J = \int (x^T Q x + u^T R u) \tag{21}$$

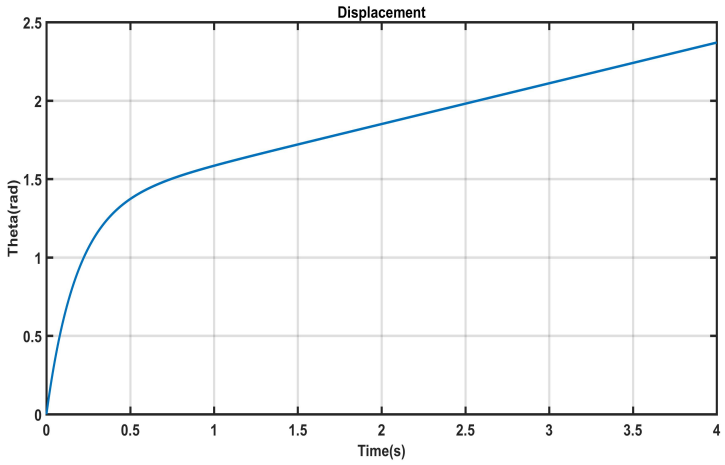

Fig. 6 LQR: Lever Displacement

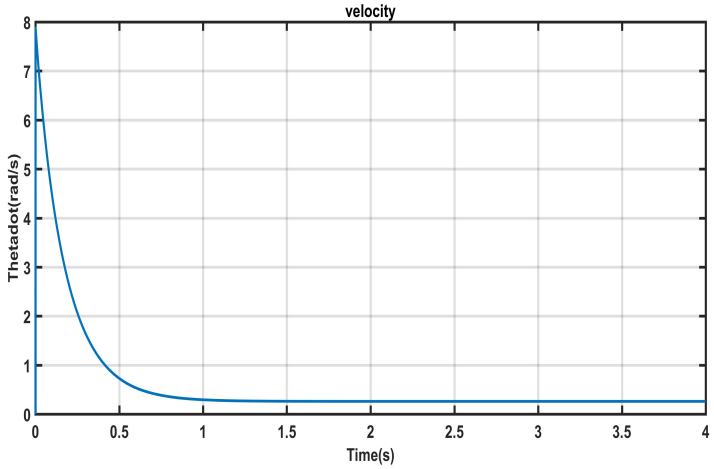

Fig. 7 LQR: Velocity

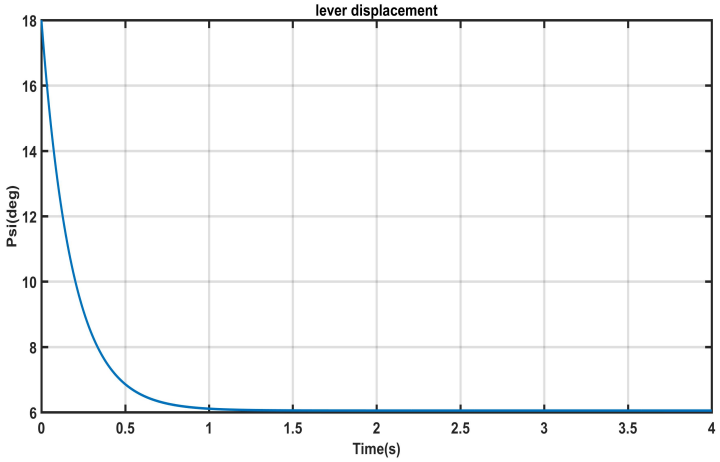

Fig. 8 LQR: Lever Displacement

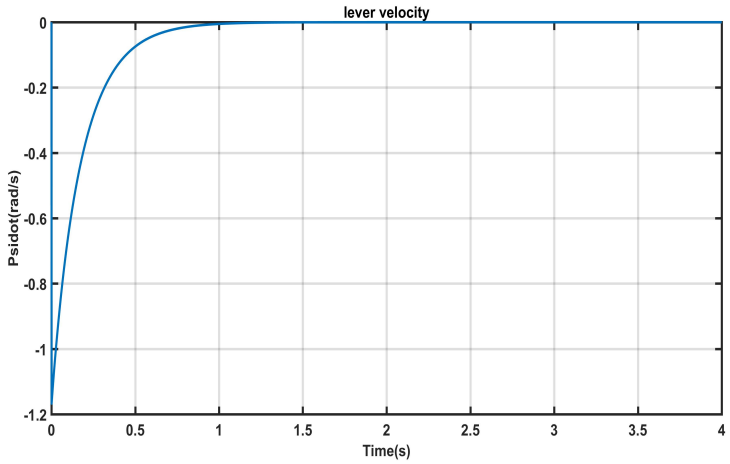

Fig. 9 LQR: Lever Velocity

In Eq. (21), Q and R are the positive semi-definite and positive symmetric matrices, respectively. The gain matrix of control law are Eq. (22):

$$\dot{x} = (A - BK)x. \tag{22}$$

The gain matrix is calculated by solving the Eq. (23):

$$K = R^{-1}B^{T}P. \tag{23}$$

In Eq. (23), P is a positive semi-definite matrix which is calculated by solving Algebraic Riccati Equation (ARE) Eq. (24)

$$A^{T}P + PA - PBR^{-1}B^{T}P + Q = 0. \tag{24}$$

System matrix A and B after linearization of the non-linear model are computed as:

$$A = \begin{bmatrix} 0 & 1 & 0 & 0 \\ 0 & -15.4409 & -8.6018 & 15.4901 \\ 0 & 0 & 0 & 1 \\ 0 & 2.4999 & 6.0160 & -2.4998 \end{bmatrix}$$

$$B = \begin{bmatrix} 0 \\ 10.6735 \\ 0 \\ -1.7225 \end{bmatrix}$$

and the weight matrices are computed by hit and trial method, which comes out to be:

$$Q = \begin{bmatrix} 6 & 0 & 0 & 0 \\ 0 & 1e8 & 0 & 0 \\ 0 & 0 & 1e6 & 0 \\ 0 & 0 & 0 & 32 \end{bmatrix} \textit{ and}$$

$$R = \begin{bmatrix} 0.001 \end{bmatrix}$$

After computing A, B, Q and R matrices, the gain value K was calculated. The desired state of the system was taken similar to PID-PID controller, for the comparison purpose. The desired values of

states (θ $\dot{\theta}$ ψ and $\dot{\psi}$) are taken as $x_d = [2.5, 0.28\ \pi/30\ 0]$ respectively. Initial condition is taken as $x_0 = [0\ 0\ \pi/10\ 0]$.The control input U is fed to the full nonlinear system after that simulation is performed, and the graphs were plotted as shown in Fig. 6, Fig. 7, Fig. 8, and Fig. 9.The following control input Eq. (25) was fed to the nonlinear system:

$$u = -K(x - x_d) \tag{25}$$

Responses of all the four state i.e. (θ, $\dot{\theta}$, ψ and $\dot{\psi}$) for LQR controlled model are plotted in Fig. 6, Fig. 7, Fig. 8, and Fig. 9, respectively. In the LQR response, (ψ) was initially taken as 18° and after few seconds it smoothly attains the desired value of 6° as shown in Fig. 8. From Fig. 8 it can be observed that the initial overshoot is due to the positive deflection of pitch angle in forwarding direction. TW-SBHT moves in the forward direction and attains the desired angle, as per the control objective. The TW-SBHT moves with constant velocity in the forward direction because pitch angle has the constant deflection of 6° in a positive direction. These simulation results justify that LQR effectively controls the TW-SBHT.

5 SDRE Controller

The SDRE control works somewhat similar to LQR control. However, the major difference between them is the formulation of state space form. In SDRE, the A and B matrices are the state dependent matrices or state-dependent coefficient matrices (SDC). The system dynamics of TW-SBHT are considered as a pseudo-linear system. The SDC matrices are not unique and there can be n number of different A and B matrices. The non-uniqueness of the SDC matrices makes the control design with a sub-optimal approach [17].There are broadly two methods to create the SDC matrices, first by factorization and secondly by computing the Jacobian of the nonlinear system. In this paper, SDC matrices are computed by Jacobian. The Jacobian method is generally used in the extended Kalman filter [18].The control methodology and algorithm are described as:

$$\dot{x} = F(x) + Bu \tag{26}$$

The nonlinear system is assumed in the form as mention in the Eq. (26) where $F(x)$ is the state vector which describes the behavior of the controller and B is the control matrix and u is the input. The system can be described as the state dependent matrices in state space form as in Eq. (27):

$$\dot{x} = A(x)x(t) + B(x)u(t) \tag{27}$$

The goal is similar to the LQR and PID controller. The cost function for SDRE controller as shown in Eq. (28) is almost similar to the LQR controller and also the performance index in quadratic form are likewise as in the previous method i.e. LQR controller.

$$J = \int (x^T Q(x)x + u^T R(x)u) \tag{28}$$

Where Q and R are the positive semi-definite and positive symmetric matrices, respectively. Moreover $x^T Q(x)x$ is the measure of the control accuracy and $u^T R(x)u$ is the measure of control effort. The Eq. (26) and Eq. (27) must satisfy the following conditions:

- F(X) and B(X) as well as Q(X) and R(X) must be continues as well as differentiable in the interested domain.
- F(0)= 0 So that in the steady state when u goes to zero then F(x) must be goes to zero. Otherwise there is compatibility issue.

- B(x)= 0 in the domain of interest.
- F(x)=A(x)x , [A(x), B(x)] must be controllable and point wise stabilize able

After computing the Jacobian of the equation of motion of the system, the A(x) and B(x) SDC matrices comes out to be $A_{22}, A_{23}, A_{24}, A_{42}, A_{43}, A_{44}, B_{21}$,and B_{41} are are mention in the Appendix A.

$$A = \begin{bmatrix} 0 & 1 & 0 & 0 \\ 0 & A_{22} & A_{23} & A_{24} \\ 0 & 0 & 0 & 1 \\ 0 & A_{42} & A_{43} & A_{44} \end{bmatrix}$$

$$B = \begin{bmatrix} 0 \\ B_{21} \\ 0 \\ B_{41} \end{bmatrix}$$

The Q and R metrics are computed as:

$$Q = \begin{bmatrix} 1 & 0 & 0 & 0 \\ 0 & 1e3 & 0 & 0 \\ 0 & 0 & 10e9 & 1 \\ 0 & 0 & 0 & 1 \end{bmatrix}$$

$$R = \begin{bmatrix} 0.000079 \end{bmatrix}$$

Now, to compute the control law of the SDRE controller, it requires to solve the state dependent algebraic Riccati equation (SDARE) (29). The SDARE gives the unique solution of the P(x) which further used in Eq. (30) to find the gain matrices K.

$$A^T(x)P(x) + P(x)A(x) - P(x)B(x)R^{-1}(x)B^T(x)P(x) + Q(x) = 0 \tag{29}$$

The P(x) is used to compute the full state feedback control law which minimizes the above cost function. The control law can be represented as:

$$u(x) = -K(x) = -R^{-1}(x)B^T(x)P(x) \tag{30}$$

After the calculation of gain matrix K , -K(x-x_d) is feed to the plant or to the dynamics of the system Eq. (2.1) and Eq. (2.1), where x_d is the desire states of the system.

5.0.1 Algorithm of the SDRE controller

- Define a small interval of time or time steps. Start with T=T_0=0.
- Put the values of all the states x=[θ $\dot{\theta}$ ψ $\dot{\psi}$] (start with the initial state x_0) into the A and B matrices and make the SDC matrices A(x) ,B(x).
- Solve the algebraic riccati and find the unique solution of the equation that is P(x).
- Substitute the value of P(x) in the control law in Eq. (30)) and compute the value of gain matrices K. Then feed the gain matrices to the equation of system Eq. (2.1) and Eq. (2.1) and after solving these equations of motion, update the value of x with the new value of states.
- After completing the above steps, increase the value of T by the step size. Iteration will end when T reaches to its final value T_f.

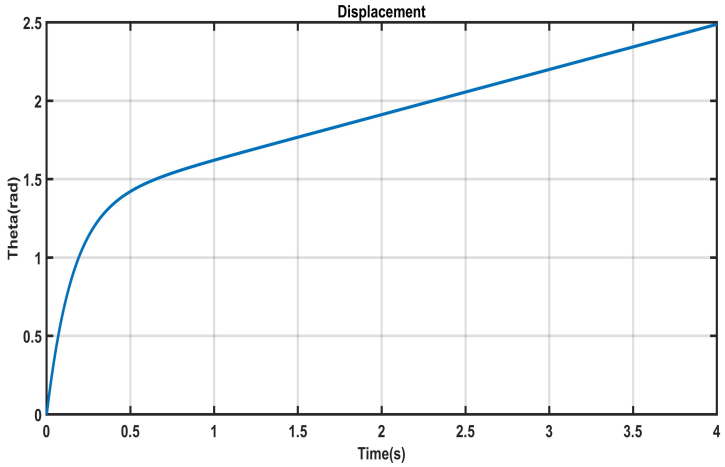

Fig. 10 SDRE: Displacement

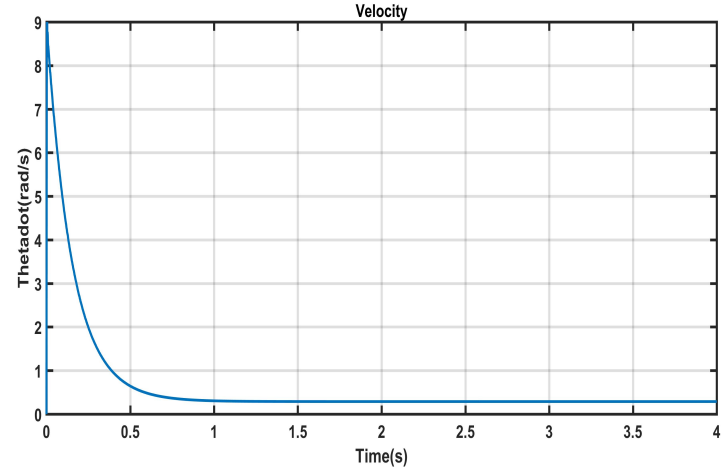

Fig. 11 SDRE: Velocity

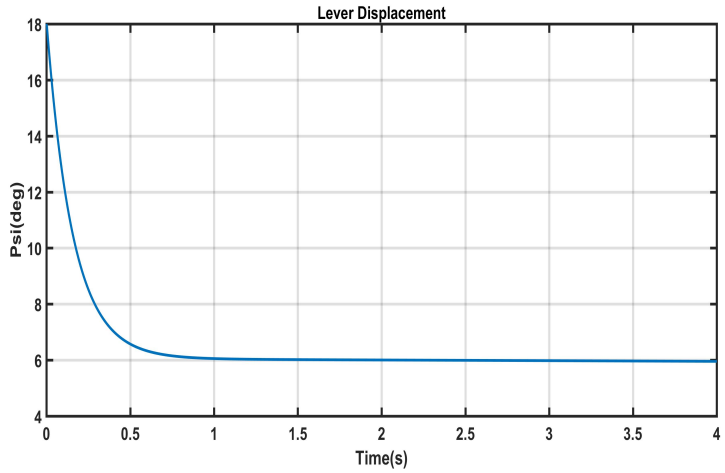

Fig. 12 SDRE: Displacement of Lever

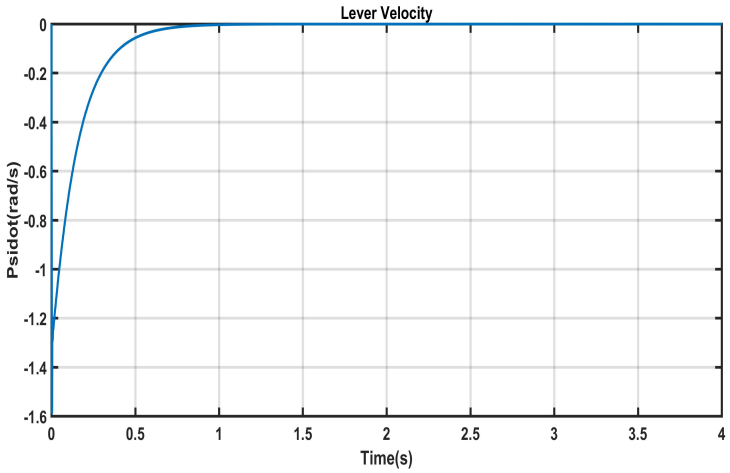

Fig. 13 SDRE: Velocity of Lever

- Decrease the step size for better accuracy.

The dynamics model of TW-SHBT was established in MATLAB software after incorporating the system dynamics presented in section (2). The model parameters Tables (2) and the reference states were kept similar for PID-PID, LQR and SDRE control schemes, for comparison purpose. The numerical simulation results for $[\theta\ \dot{\theta}\ \psi\ \dot{\psi}]$, for TW-SBHT based on SDRE control, are shown in Fig. 10, Fig. 11, Fig. 12 and Fig. 13,respectively. The initial conditions were $x_0 = [0, 0, \pi/10, 0]$ and the desire states are $x_d = [2.5, 0.28, \pi/30, 0]$.From Fig. 12, it can be clearly seen that the initial deflection of the lever (which was 18°) quickly converge to reference angles of 6°.Therefore, it can be claimed that the SDRE controller can stabilize the system at a faster rate for the given reference. Similarly, for the velocity of TW-SBHT ($\dot{\theta}$) Fig. 11, it can be observed that the TW-SBHT stabilizes at the given reference speed of 0.28 rad/sec from a sudden increase in the speed due to the large initial deflection in the lever. It maintains the constant speed to the corresponding deflection of 6° in the forward direction. The results for the velocity of lever and displacement of the TW-SBHT are in accordance with the displacement of lever and velocity of TW-SBHT, respectively.

6 Comparisosn of Performance of PID-PID, LQR and SDRE

The performance comparison of PID-PID, LQR and SDRE controllers for velocity ($\dot{\theta}$) and displacement of the lever (ψ) is shown in Fig. 14 and Fig. 15, respectively. Table (3) represents the comparison of controllers in terms of settling time, steady-state error and decay time for the velocity of TW-SBHT (data is fetched from Fig. 14). The data from the Table (3) clearly shows that SDRE responds more rapidly than the LQR and PID controller.SDRE settles the velocity of the TW-SBHT ($\dot{\theta}$) 2% faster than the PID-PID controller and 14% faster than the LQR controller.

Table 3 Performance comparison PID, LQR and SDRE $\dot{\theta}$

Parameter	PID-PID	LQR	SDRE
Settling time(s)	0.6025	0.6888	0.5911
Steady state error	0.1%	3.5%	2.6%
Decay Time	0.383	0.389	0.3412

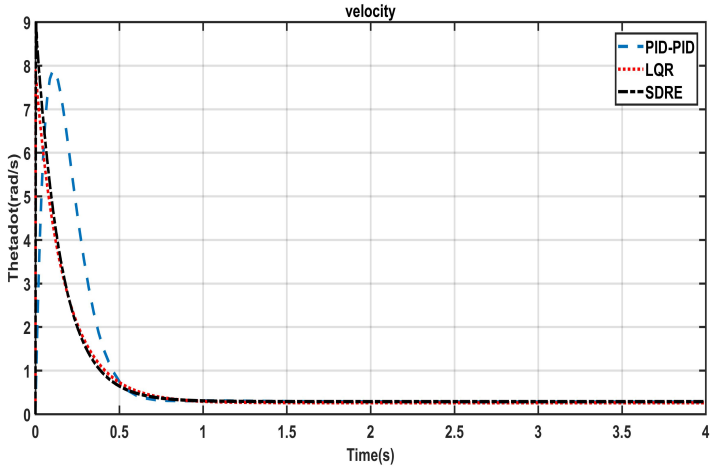

Fig. 14 Comparison of velocity

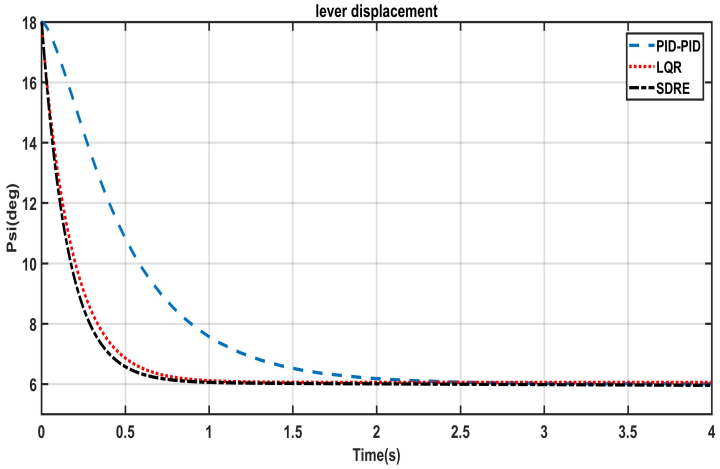

Fig. 15 Comparison of Lever Displacement

Table 4 Performance comparison PID, LQR and SDRE ψ

Parameter	PID-PID	LQR	SDRE
Settling time(s)	1.0170	0.4147	0.3550
Steady state error	0.1 %	0.84%	0.75 %
Decay time	1.1138	0.415	0.355

6.1 Stability Analysis

In this section, the ability of all the three controllers to maintain the stability of the lever angle or the pitch angle at the upright position is analyzed. The step input was kept in the nonlinear region of large pitch angle which occurred due to the external disturbance7. The step input is kept at 12.8 deg. for 0.01 sec From Fig16 it can be claimed that the SDRE controller removes the external disturbance more effectively than the LQR and PID-PID controllers. Furthermore, the stability also analysis with the pulse disturbance as shown in Fig.17. In the pulse disturbance, the amplitude is kept at 9 deg. for

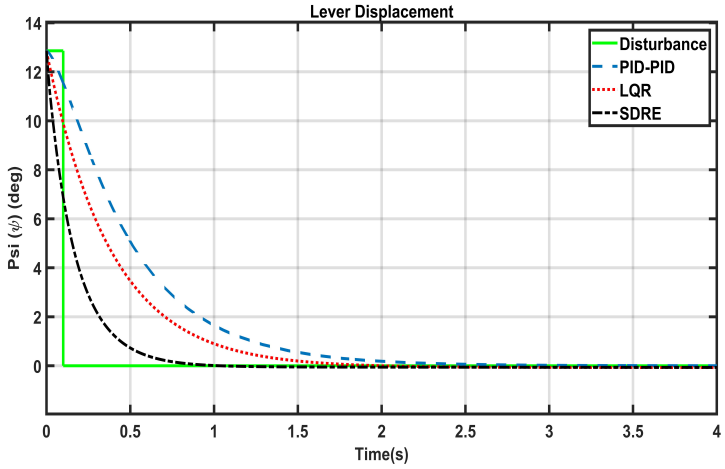

Fig. 16 Comparison under external disturbance

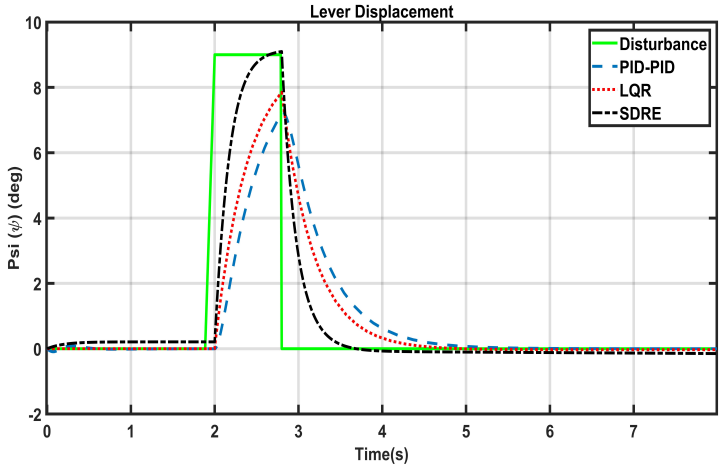

Fig. 17 Comparison under Pulse Disturbance

10% time of the simulation i.e. from 2.0 sec to 2.8 sec. Even in this case SDRE controller attenuate the disturbance more quickly as compared to the LQR and PID-PID controller.

7 Conclusion

This paper presents the mathematical modeling and control of the two-wheeled self-balancing human transporter. The equations of motions of the system are derived using the Lagrangian Mechanics. The control objective was to stabilize the velocity of the TW-SBHT for deflection of the lever of the vehicle. Different controllers viz. PID-PID, LQR, and SDRE were implemented on the TW-SBHT and all the three control schemes successfully conquered the control objective and converge the TW-SBHT to its desired states. The response of the PID-PID, LQR and SDRE controller is analysed based on the settling time, steady state error and decay time. The results show that the SDRE controller has better performance for controlling the TW-SBHT as compared to the LQR and PID-PID controller.

APPENDIX

Elements of SDC matrices

$$A_{22} = -(2J_b b + 2J_b f_w + 2L^2 Mb + 2L^2 Mf_w + 4J_m f_w n^2 + 2LMR_w bcos(\psi))/(2J_b J_w +$$
$$L^2 M^2 R_w^2 + 2J_w L^2 M + J_b MR_w^2 + 2J_b J_m n^2 + 4J_m J_w n^2 + 2J_b R_w^2 m + 2J_m L^2 Mn^2 +$$
$$2J_m MR_w^2 n^2 + 2L^2 MR_w^2 m + 4J_m R_w^2 mn^2 - L^2 M^2 R_w^2 cos(\psi)^2 + 4J_m LMR_w n^2 cos(\psi))$$

$$A_{23} = (L^3 M^2 R_w \dot{\psi}^2 cos(\psi) - L^2 M^2 R_w gcos(\psi)^2 + L^2 M^2 R_w gsin(\psi)^2 - 2LMR_w b\dot{\psi}sin(\psi) + 2LMR_w b\dot{\theta}sin(\psi)$$
$$+J_b LMR_w \dot{\psi}^2 cos(\psi) + 2J_m LMgn^2 cos(\psi) - LMR_w Vasi(\psi) + 2J_m LMR_w n^2 \dot{\psi}^2 cos(\psi))/(2J_b J_w$$
$$+L^2 M^2 R_w^2 + 2J_w L^2 M + J_b MR_w^2 + 2J_b J_m n^2 + 4J_m J_w n^2 + 2J_b R_w^2 m + 2J_m L^2 Mn^2 + 2J_m MR_w^2 n^2$$
$$+2L^2 MR_w^2 m + 4J_m R_w^2 mn^2 - L^2 M^2 R_w^2 cos(\psi)^2 + 4J_m LMR_w n^2 cos(\psi)$$
$$-2cos(\psi)sin(\psi)L^2 M^2 R_w^2 - 4J_m sin(\psi)LMR_w n^2)$$
$$(J_b Va + 2J_b b\dot{\psi} - 2J_b b\dot{\theta} - 2J_b f_w \dot{\theta} + L^2 MVa + 2L^2 Mb\dot{\psi}$$
$$-2L^2 Mb\dot{\theta} - 2L^2 Mf_w \dot{\theta} - 4J_m f_w n^2 \dot{\theta} + L^3 M^2 R_w \dot{\psi}^2 sin(\psi)$$
$$-L^2 M^2 R_w gcos(\psi)sin(\psi) + J_b LMR_w \dot{\psi}^2 sin(\psi) + 2J_m LMgn^2 sin(\psi)$$
$$+LMR_w Vacos(\psi) + 2LMR_w b\dot{\psi}cos(\psi) - 2LMR_w b\dot{\theta}cos(\psi) + 2J_m LMR_w n^2 \dot{\psi}^2 sin(\psi))/(2J_b J_w + L^2 M^2 R_w^2 +$$
$$2J_w L^2 M + J_b MR_w^2 + 2J_b J_m n^2 + 4J_m J_w n^2 + 2J_b R_w^2 m$$
$$+2J_m L^2 Mn^2 + 2J_m MR_w^2 n^2 + 2L^2 MR_w^2 m + 4J_m R_w^2 mn^2 - L^2 M^2 R_w^2 cos(\psi)^2 + 4J_m LMR_w n^2 cos(\psi)^2.$$

$$A_{24} = (2J_b b + 2L^2 Mb + 2L^3 M^2 R_w \dot{\psi}sin{>}\psi) + 2LMR_w bcos{>}\psi) + 2J_b LMR_w \dot{\psi}sin{>}\psi) +$$
$$4J_m LMR_w n^2 \dot{\psi}sin{>}\psi))/(2J_b J_w + L^2 M^2 R_w^2 + 2J_w L^2 M + J_b MR_w^2 + 2J_b J_m n^2 + 4J_m J_w n^2 + 2J_b R_w^2 m +$$
$$2J_m L^2 Mn^2 + 2J_m MR_w^2 n^2 + 2L^2 MR_w^2 m + 4J_m R_w^2 mn^2 - L^2 M^2 R_w^2 cos{>}\psi)r2 + 4J_m LMR_w n^2 cos{>}\psi))$$

$$A_{42} = (4J_w b + 2MR_w^2 b - 4J_m f_w n^2 + 4R_w^2 bm + 2LMR_w bcos{>}\psi) + 2LMR_w f_w cos{>}\psi))/(2JbJ_w +$$
$$L^2 M^2 R_w^2 + 2J_w L^2 M + J_b MR_w^2 + 2J_b J_m n^2 + 4J_m J_w n^2 + 2J_b R_w^2 m +$$
$$2J_m L^2 Mn^2 + 2J_m MR_w^2 n^2 + 2L^2 MR_w^2 m + 4J_m R_w^2 mn^2 - L^2 M^2 R_w^2 os{>}\psi)r2 + 4J_m LMR_w n^2 cos{>}\psi))$$

$$A_{43} = (LM^2 R_w^2 gcos(\psi) - L^2 M^2 R_w^2 \dot{\psi}^2 cos(\psi)^2 + L^2 M^2 R_w^2 \dot{\psi}^2 sin(\psi)^2 + 2J_w LMgcos(\psi) +$$
$$2LMR_w b\dot{\psi}sin(\psi) - 2LMR_w b\dot{\theta}sin(\psi) - 2LMR_w f_w \dot{\theta}sin(\psi) + 2J_m LMgn^2 cos(\psi) +$$
$$2LMR_w^2 gmcos(\psi) + LMR_w Vasin(\psi) + 2J_m LMR_w n^2 \dot{\psi}^2 cos(\psi))/(2J_b J_w +$$
$$L^2 M^2 R_w^2 + 2J_w L^2 M + J_b MR_w^2 + 2J_b J_m n^2 + 4J_m J_w n^2 +$$
$$2J_b R_w^2 m + 2J_m L^2 Mn^2 + 2J_m MR_w^2 n^2 + 2L^2 MR_w^2 m +$$
$$4J_m R_w^2 mn^2 - L^2 M^2 R_w^2 cos(\psi)^2 + 4J_m LMR_w n^2 cos(\psi)) +$$
$$((2cos(\psi)sin(\psi)L^2 M^2 R_w^2 - 4J_m sin(\psi)LMR_w n^2)(2J_w Va + 4J_w b\dot{\psi} - 4J_w b\dot{\theta}$$
$$+MR_w^2 Va + 2MR_w^2 b\dot{\psi} - 2MR_w^2 b\dot{\theta} + 2R_w^2 Vam + 4R_w^2 bm\dot{\psi} +$$
$$4J_m f_w n^2 \dot{\theta} - 4R_w^2 bm\dot{\theta} - LM^2 R_w^2 gsin(\psi) -$$
$$2J_w LMgsin(\psi) - 2J_m LMgn^2 sin(\psi) - 2LMR_w^2 gmsin(\psi) + LMR_w Vacos(\psi)$$

$$+L^2M^2R_w^2\dot{\psi}^2cos(\psi)sin(\psi)+2LMR_wb\dot{\psi}cos(\psi)$$
$$-2LMR_wb\dot{\theta}cos(\psi)-2LMR_wf_w\dot{\theta}cos(\psi)-2J_mLMR_wn^2\dot{\psi}^2sin(\psi)))/(2J_bJ_w+$$
$$L^2M^2R_w^2+2J_wL^2M+J_bMR_w^2+2J_bJ_mn^2+4J_mJ_wn^2+2J_bR_w^2m+2J_mL^2Mn^2+$$
$$2J_mMR_w^2n^2+2L^2MR_w^2m+4J_mR_w^2mn^2-L^2M^2R_w^2cos(\psi)^2+4J_mLMR_wn^2cos(\psi))^2$$
$$A_{44}=-(2\dot{\psi}cos(\psi)sin(\psi)L^2M^2R_w^2-4J_m\dot{\psi}sin(\psi)LMR_wn^2$$
$$+2bcos(\psi)LMR_w+2bMR_w^2+4bmR_w^2+4J_wb)/(2J_bJ_w+L^2M^2R_w^2$$
$$+2J_wL^2M+J_bMR_w^2+2J_bJ_mn^2+4J_mJ_wn^2+$$
$$2J_bR_w^2m+2J_mL^2Mn^2+2J_mMR_w^2n^2+2L^2MR_w^2m+4J_mR_w^2mn^2-$$
$$L^2M^2R_w^2cos(\psi)^2+4J_mLMR_wn^2cos(\psi))]$$
$$B_{21}=(MaL^2+MR_wacos>\psi)L+J_ba)/(2J_bJ_w+L^2M^2R_w^2+2J_wL^2M+$$
$$J_bMR_w^2+2J_bJ_mn^2+4J_mJ_wn^2+2J_bR_w^2m+2J_mL^2Mn^2+2J_mMR_w^2n^2+$$
$$2L^2MR_w^2m+4J_mR_w^2mn^2-L^2M^2R_w^2os>\psi)r2+4J_mLMR_wn^2cos>\psi))$$
$$B_{41}=-(2J_wa+MR_w^2a+2R_w^2am+LMR_wacos(\psi))/(2J_bJ_w+L^2M^2R_w^2$$
$$+2J_wL^2M+J_bMR_w^2+2J_bJ_mn^2+4J_mJ_wn^2+2J_bR_w^2m+2J_mL^2Mn^2+2J_mMR_w^2n^2+2L^2MR_w^2m+$$
$$4J_mR_w^2mn^2-L^2M^2R_w^2cos(\psi)^2+4J_mLMR_wn^2cos(\psi))]$$

References

[1] Shimizu, Y., and Shimada, A. (2010). Direct tilt angle control on inverted pendulum mobile robots. In 2010 11th IEEE International Workshop on Advanced Motion Control (AMC) (pp. 234-239). IEEE.

[2] Lin, S. C., and Tsai, C. C. (2008). Development of a self-balancing human transportation vehicle for the teaching of feedback control. IEEE Transactions on Education, 52(1), 157-168

[3] Lupian, L. F., and Avila, R. (2008, October). Stabilization of a wheeled inverted pendulum by a continuous-time infinite-horizon LQG optimal controller. In 2008 IEEE Latin American Robotic Symposium (pp. 65-70). IEEE.

[4] Huang, J., Guan, Z. H., Matsuno, T., Fukuda, T., and Sekiyama, K. (2010). Sliding-mode velocity control of mobile-wheeled inverted-pendulum systems. IEEE Transactions on robotics, 26(4), 750-758.

[5] Irfan, S., Mehmood, A., Razzaq, M. T., and Iqbal, J. (2018). Advanced sliding mode control techniques for inverted pendulum: Modelling and simulation. Engineering science and technology, an international journal, 21(4), 753-759.

[6] Lin, S. C., Tsai, C. C., and Huang, H. C. (2011). Adaptive robust self-balancing and steering of a two-wheeled human transportation vehicle. Journal of Intelligent and Robotic Systems, 62(1), 103-123.

[7] Kim, S., and Kwon, S. (2017). Nonlinear optimal control design for underactuated two-wheeled inverted pendulum mobile platform. IEEE/ASME Transactions on Mechatronics, 22(6), 2803-2808.

[8] Xu, J. X., Guo, Z. Q., and Lee, T. H. (2013). Design and implementation of integral sliding-mode control on an underactuated two-wheeled mobile robot. IEEE Transactions on industrial electronics, 61(7), 3671-3681. .

[9] Li, Z., and Yang, C. (2011). Neural-adaptive output feedback control of a class of transportation vehicles based on wheeled inverted pendulum models. IEEE Transactions on Control Systems Technology, 20(6), 1583-1591.

[10] Huang, C. H., Wang, W. J., and Chiu, C. H. (2010). Design and implementation of fuzzy control on a two-wheel inverted pendulum. IEEE Transactions on Industrial Electronics, 58(7), 2988-3001.

[11] Jadlovska, S., and Sarnovsky, J. (2013, September). Application of the state dependent Riccati equation method in nonlinear control design for inverted pendulum systems. In 2013 IEEE 11th International Symposium on Intelligent Systems and Informatics (SISY) (pp. 209-214). IEEE.

[12] Cimen, T. (2012). Survey of state dependent Riccati equation in nonlinear optimal feedback control synthesis. Journal of Guidance, Control, and Dynamics, 35(4), 1025-1047.

[13] Yamamoto, Y. (2008). NXTway-GS Model-Based Design-Control of self-balancing two-wheeled robot built with LEGO Mindstorms NXT. Cybernet Systems Co., Ltd.

[14] Arvidsson, M., and Karlsson, J. (2012). Design, construction and verification of a self-balancing vehicle.
[15] Kim, S., and Kwon, S. (2015). Dynamic modeling of a two-wheeled inverted pendulum balancing mobile robot. International Journal of Control, Automation and Systems, 13(4), 926-933..
[16] van Rensburg, R., Steyn, N., Trenoras, L., Hamam, Y., and Monacelli, E. (2017). Stability and enhancement analysis of a modelled self-balancing verticalized mobility aid using optimal control techniques. African Journal of Science, Technology, Innovation and Development, 9(1), 93-109.
[17] Batmani, Y., Davoodi, M., and Meskin, N. (2016). Nonlinear suboptimal tracking controller design using state dependent Riccati equation technique. IEEE Transactions on Control Systems Technology, 25(5), 1833-1839.
[18] Prach, A. N. N. A. (2015). Faux Riccati equation techniques for feedback control of nonlinear and time-varying systems(Doctoral dissertation, PhD. Thesis. School of Natural and Applied Sciences. Aerospace Engineering. Middle East Technical University).